Superconductor
Science and
Technology

PURPOSE-LED
PUBLISHING™

PAPER • **OPEN ACCESS**

Enhancement of superconducting state properties of $Fe_{0.994}Ni_{0.007}Te_{0.66}Se_{0.34}$ single crystal with increasing pressure: a correlation with pressure-induced crystallinity degradation

To cite this article: Jaroslaw Pietosa *et al* 2020 *Supercond. Sci. Technol.* **33** 045004

View the article online for updates and enhancements.

You may also like

- Single-crystal growth of the iron-based superconductor $La_{0.34}Na_{0.66}Fe_2As_2$
Yanhong Gu, Jia-Ou Wang, Xiaoyan Ma et al.
- Interplay between magnetism and superconductivity in iron-chalcogenide superconductors: crystal growth and characterizations
Jinsheng Wen, Guangyong Xu, Genda Gu et al.
- Microstructural and transport properties of superconducting $FeTe_{0.65}Se_{0.35}$ crystals
A G Sivakov, S I Bondarenko, A I Prokhvatilov et al.

This content was downloaded from IP address 158.69.200.216 on 10/11/2026 at 07:17

OPEN ACCESS
IOP Publishing
Superconductor Science and Technology
Supercond. Sci. Technol. 33 (2020) 045004 (10pp)
https://doi.org/10.1088/1361-6668/ab6dc4

Enhancement of superconducting state properties of $Fe_{0.994}Ni_{0.007}Te_{0.66}Se_{0.34}$ single crystal with increasing pressure: a correlation with pressure-induced crystallinity degradation

Jaroslaw Pietosa[1], Roman Puzniak[1], Damian Paliwoda[1], Wojciech Paszkowicz[1], Andrzej Katrusiak[2], Radosław Kamiński[3], Dariusz J Gawryluk[1,4] and Andrzej Wisniewski[1]

[1] Institute of Physics, Polish Academy of Sciences, Aleja Lotników 32/46, PL-02668 Warsaw, Poland
[2] Faculty of Chemistry, Adam Mickiewicz University, Umultowska 89b, PL-61614 Poznań, Poland
[3] Department of Chemistry, University of Warsaw, Żwirki i Wigury 101, PL-02089 Warsaw, Poland
[4] Laboratory for Multiscale Materials Experiments, Paul Scherrer Institute, CH-5232 Villigen, PSI, Switzerland

E-mail: pietosa@ifpan.edu.pl

Received 16 July 2019, revised 23 December 2019
Accepted for publication 20 January 2020
Published 19 February 2020

Abstract

Detailed investigations of Ni substituted $Fe_{0.994}Ni_{0.007}Te_{0.66}Se_{0.34}$ and unsubstituted $Fe_{0.99}Te_{0.66}Se_{0.34}$ crystals were performed at ambient pressure and under hydrostatic pressure in order to understand the complex relationship between structure, magnetism, and superconductivity in iron selenides. The aim of the investigations was to determine the structural and superconducting state properties and study their evolution under pressure, up to 11 kbar. A comparison of $Fe_{0.99}Te_{0.66}Se_{0.34}$, a material with much less developed phase separation, with $FeTe_{0.5}Se_{0.5}$, a material exhibiting pronounced nanoscale phase separation, was also performed. Under ambient pressure, a weakening of superconducting state properties was observed in the $Fe_{0.994}Ni_{0.007}Te_{0.66}Se_{0.34}$ crystal, with disorder introduced by Ni substitution, as compared with those in $Fe_{0.99}Te_{0.66}Se_{0.34}$. For $Fe_{0.994}Ni_{0.007}Te_{0.66}Se_{0.34}$, the x-ray diffraction studies have revealed a degradation of crystal quality under applied elevated pressure. Superconducting state properties of the single phase $Fe_{0.99}Te_{0.66}Se_{0.34}$ crystal, such as upper and lower critical fields, were found to be poorer, at both ambient and hydrostatic pressure, than those observed for $FeTe_{0.5}Se_{0.5}$ crystals exhibiting pronounced nanoscale phase separation. Comprehensive studies of the impact of pressure on crystal structure and on superconducting state properties confirm that enhancement of superconductivity correlates with the appearance of mosaicity under pressure. The above observation leads to the expectation of a pressure-induced increase in inhomogeneity, leading to the enhancement of superconducting properties in other sulpho-iron seleno-tellurides of anti-PbO-type structure.

Keywords: superconductors, Fe–Te–Se system, single-crystal x-ray diffraction studies, thermodynamic properties, hydrostatic pressure

(Some figures may appear in colour only in the online journal)

 © 2020 The Author(s). Published by IOP Publishing Ltd Printed in the UK

This is an open access article distributed under the terms of the Creative Commons Attribution 4.0 License.
Any further distribution of this work must maintain attribution to the author(s) and the title of the work, journal citation and DOI.

1. Introduction

The discovery of superconductivity in layered iron chalcogenides of general formula Fe(Se,*Ch*) ('11'-type compounds, where Ch = S, Te) has prompted detailed studies of metal chalcogenides [1]. Research efforts have mainly concentrated on understanding the mechanism of superconductivity and on increasing the critical temperature, T_c. Within the '11' group, pure FeSe has the simplest structure (anti-α PbO type, space group $P4/nmm$ [1–3]), among the studied iron-based compounds, with $T_c < 8$ K [1], which increases up to ~14 K (in $FeTe_{1-x}Se_x$, $x = 0.5$) upon the partial substitution of a larger tellurium ion at the Se site [2, 4, 5]. Iron-chalcogenide superconductors show potential for applications in high magnetic fields, both because of a high upper critical field, H_{c2}, and a low anisotropy [6–8]. Moreover, the insignificant toxicity of their starting components, in comparison with that of the FeAs-based superconductors, simplifies its handling and therefore these compounds are considered to be promising for applications such as wires, tapes, and thin films [9–12]. Since the possibility of T_c enhancement by quantum confinement in ultrathin films [13–18] and the discovery of topological superconductivity in $FeTe_{1-x}Se_x$ systems [19] the field of possible applications has increased tremendously.

Under hydrostatic pressure an enhancement of the main superconducting parameters (T_c, lower and upper critical fields, H_{c1} and H_{c2}, critical current density, j_c) is observed for $FeTe_{0.5}Se_{0.5}$ [20]. It is worth pointing out that single crystals of $FeTe_{0.5}Se_{0.5}$ tend to exhibit a coexistence of two tetragonal phases [5, 21, 22] with nanometer-sized areas, with hexagonal symmetry inside the host matrix with tetragonal symmetry. Chemical disorder manifesting as an inhomogeneous distribution of Te/Se ions in the crystal lattice, and Fe-deficient bands hundreds of nanometers in size, is also observed [23, 24]. The results of our earlier studies performed on $FeTe_{0.65}Se_{0.35}$ suggested that an inhomogeneity is an intrinsic property of $FeTe_{1-x}Se_x$ superconductors [24], which agrees with earlier electron energy loss spectroscopy (EELS) analysis, indicating the importance of an inhomogeneous anion distribution [25]. As a summary of the cited study, it was pointed out that phase separation, manifesting itself through inhomogeneous ion distribution and through the presence of nanosized hexagonal regions, enhances the superconductivity in chalcogenides [24]. Importantly, the $FeTe_{0.65}Se_{0.35}$, with lower Se content and slightly lowered critical temperature (12.9 K) than that of $FeTe_{0.5}Se_{0.5}$, has been reported to exhibit much less pronounced nanoscale phase separation and to behave almost like a single-phase crystal [23, 24].

Establishing a relationship between the structure, magnetism and superconductivity in iron chalcogenides is a very relevant issue as was stressed already by many authors; see, for example, early and later reviews and references in [26–28]. Taking the above into account, we decided to perform detailed crystallographic and magnetic investigations into Ni substituted $Fe_{0.994}Ni_{0.007}Te_{0.66}Se_{0.34}$ [23, 29–31] in order to determine structural and superconducting state properties and to study their evolution, comparing a material exhibiting pronounced nanoscale phase separation ($FeTe_{0.5}Se_{0.5}$) with a material with much less developed phase separation ($Fe_{0.99}Te_{0.66}Se_{0.34}$). In this work, we study the impact of external hydrostatic pressure on the intrinsic and extrinsic superconducting state properties for the $Fe_{0.99}Te_{0.66}Se_{0.34}$ sample, together with the one with partial replacement of Fe by Ni ions, i.e. $Fe_{0.994}Ni_{0.007}Te_{0.66}Se_{0.34}$, both of them grown as a single-phase crystal [23]. We show for both compounds a weakening of superconducting-state properties as a result of decreasing the selenium content from $x = 0.5$ to 0.34, and the enhancement of these properties under hydrostatic pressure, despite weakening them by chemical pressure. We correlate changes in the superconducting-state properties with the evolution of crystal quality by means of x-ray diffraction under hydrostatic pressure performed for $Fe_{0.994}Ni_{0.007}Te_{0.66}Se_{0.34}$.

2. Details of synthesis and experiment

Single crystals of nominal composition of $FeTe_{0.65}Se_{0.35}$ and $Fe_{0.995}Ni_{0.005}Te_{0.65}Se_{0.35}$ were grown by the vertical Bridgman method. Stoichiometric quantities of iron chips (3N5), tellurium powder (4N), selenium powder (pure) and NiSe (pure) were used to prepare the crystals. The starting materials were weighed, mixed and stored in argon atmosphere in a glove box. Evacuated sealed quartz ampoules with double walls containing starting materials were located in a furnace with an axial temperature gradient of 1.6 °C mm^{-1}. The thermal conditions of synthesis and crystal growth were as follows: the ingot was heated for 3 h at 730 °C, then the temperature was increased to 920 °C. After melting, this temperature was maintained for 3 h, then the samples were cooled down to 500 °C at a rate of 5 °C h^{-1}, then to 200 °C at a rate of 60 °C h^{-1}, and finally cooled down to room temperature [23]. The resulting single crystals exhibit well developed (001) natural planes, corresponding to cleavage planes of a PbO type structure.

The quantitative point analysis, using field emission scanning electron microscope (FESEM) JEOL JSM-7600F operating at 20 kV incident energy, coupled with the Oxford INCA energy dispersive x-ray spectroscope (EDX), was performed on the cleavage planes of the crystals. The average chemical composition of the matrices of the studied samples determined by SEM/EDX analysis is $Fe_{0.99}Te_{0.66}Se_{0.34}$ and $Fe_{0.994}Ni_{0.007}Te_{0.66}Se_{0.34}$ with an accuracy of ±0.02. Later in the text we will refer to the crystals' average composition, not the nominal one. All details concerning the structure of the studied samples were published in our earlier papers [23, 24]. A photograph of the crystal with identical nominal composition to that studied in the current manuscript is shown in figure 4(c) of [23].

X-ray diffraction measurements of $Fe_{0.99}Te_{0.66}Se_{0.34}$ and $Fe_{0.994}Ni_{0.007}Te_{0.66}Se_{0.34}$ single crystals were performed using Xcalibur S2 Agilent diffractometers equipped with a CCD detector and a monochromated Mo sealed tube source. Both $Fe_{0.99}Te_{0.66}Se_{0.34}$ and $Fe_{0.994}Ni_{0.007}Te_{0.66}Se_{0.34}$ crystals were measured at room temperature at ambient pressure. A

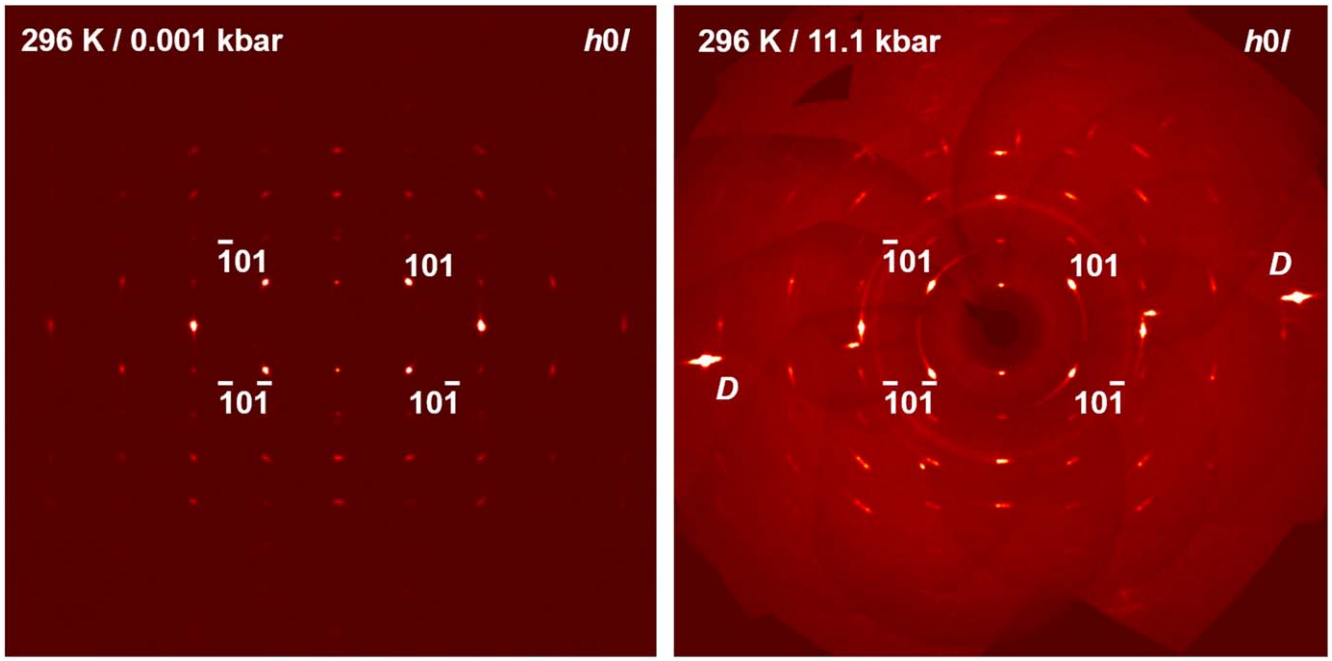


Figure 1. *h0l* layer of $Fe_{0.994}Ni_{0.007}Te_{0.66}Se_{0.34}$ crystal measured at room temperature under ambient and nonambient pressure. Left panel presents the data obtained at ambient pressure. Data presented in the right panel were obtained for a crystal enclosed in a modified Merrill–Bassett diamond-anvil at 11.1 kbar; here the reflections from diamond-anvil crystals are additionally present (those denoted by '*D*').

high pressure experiment employing a modified Merrill–Bassett diamond-anvil cell [32] (DAC with the anvils mounted directly on Inconel supports) has been performed for the $Fe_{0.994}Ni_{0.007}Te_{0.66}Se_{0.34}$ single crystal at 11.1 kbar at room temperature. The studied single crystal was glued to the culet surface of the first diamond anvil together with a small ruby chip and placed in a 0.3 mm diameter hole of a 0.1 mm thick tungsten gasket. The chamber was filled with hydrostatic pressure-transmitting medium (silicon oil) and closed. A semi-automatic gasket-shadowing procedure [33] was used for DAC centering along the x-ray beam. The CrysAlisPro program suite was used for the data collection, orientation-matrix determination, and initial data reduction.

Magnetic measurements of a $Fe_{0.99}Te_{0.66}Se_{0.34}$ single crystal, with the dimensions $a = 0.12$ cm and $b = 0.12$ cm in the *ab*-plane and with a thickness of 0.053 cm along the *c*-axis, and a single crystal of $Fe_{0.994}Ni_{0.007}Te_{0.66}Se_{0.34}$, with the dimensions $a = 0.10$ cm and $b = 0.11$ cm in the *ab*-plane and with a thickness of 0.095 cm along the *c*-axis, were performed by means of a Quantum Design superconducting quantum interference device magnetometer. A magnetic field, of up to 50 kOe, was oriented parallel to the *c*-axis of the crystal. Hydrostatic pressure was applied, by means of an easyLab Technologies MCell10 pressure cell with Daphne 7373 oil [34], which is recognized as the optimal pressure media providing the smallest decrease in pressure with lowering temperature for pressures above 7 kbar [35]. A high-purity Sn wire was used as an *in situ* manometer. The background signal coming from the pressure cell was subtracted based on measurements performed under ambient pressure for the sample mounted (i) directly on the diffractometer stage and (ii) mounted inside the pressure cell.

3. Results and discussion

3.1. X-ray diffraction studies

For a set of $FeTe_{0.65}Se_{0.35}$ single crystals [23], the narrowest transition from normal to the superconducting state (width ~0.6 K) has been observed for a sample exhibiting the largest noticed value of $\Delta\omega$ equal to $6'$ for the 004 rocking curve. Additionally, the decrease in the $\Delta\omega$ value was associated with the increase in the width of the transition (90%–10% criterion) [23]. In order to better understand the possible connection between the crystal inhomogeneity and superconducting properties, we decided to investigate the $Fe_{0.994}Ni_{0.007}Te_{0.66}Se_{0.34}$ sample with $\Delta\omega = 5.7'$ [23].

The crystal structure of $Fe_{0.994}Ni_{0.007}Te_{0.66}Se_{0.34}$ was identified as that of the anti-PbO type, but the quality was insufficient for studies of structure details. Identification of this phase is in line with the results of studies using x-ray diffraction [36, 37] and other methods [38–40], showing that the anti-PbO phase is stable in systems of close chemical composition at pressures of up to at least ~25 kbar. After application of pressure, the shape of diffraction spots changed: the roughly circular spots became extended along a direction corresponding to the run of Debye–Scherrer rings (figure 1), which is most likely caused by pressure-induced mosaicity increase of the sample. For the diffraction-spot shape analysis we selected the strong 101 and $10\bar{1}$ reflections. After application of pressure, the first of them is elongated by a factor of 1.22, the second one by a factor of 1.78. The quoted reflection extension was calculated, using contour maps (those presented in figure 2) at the level of 50% of peak height. Apparently, there is no peak broadening in the radial direction, showing that application of pressure does not influence the chemical

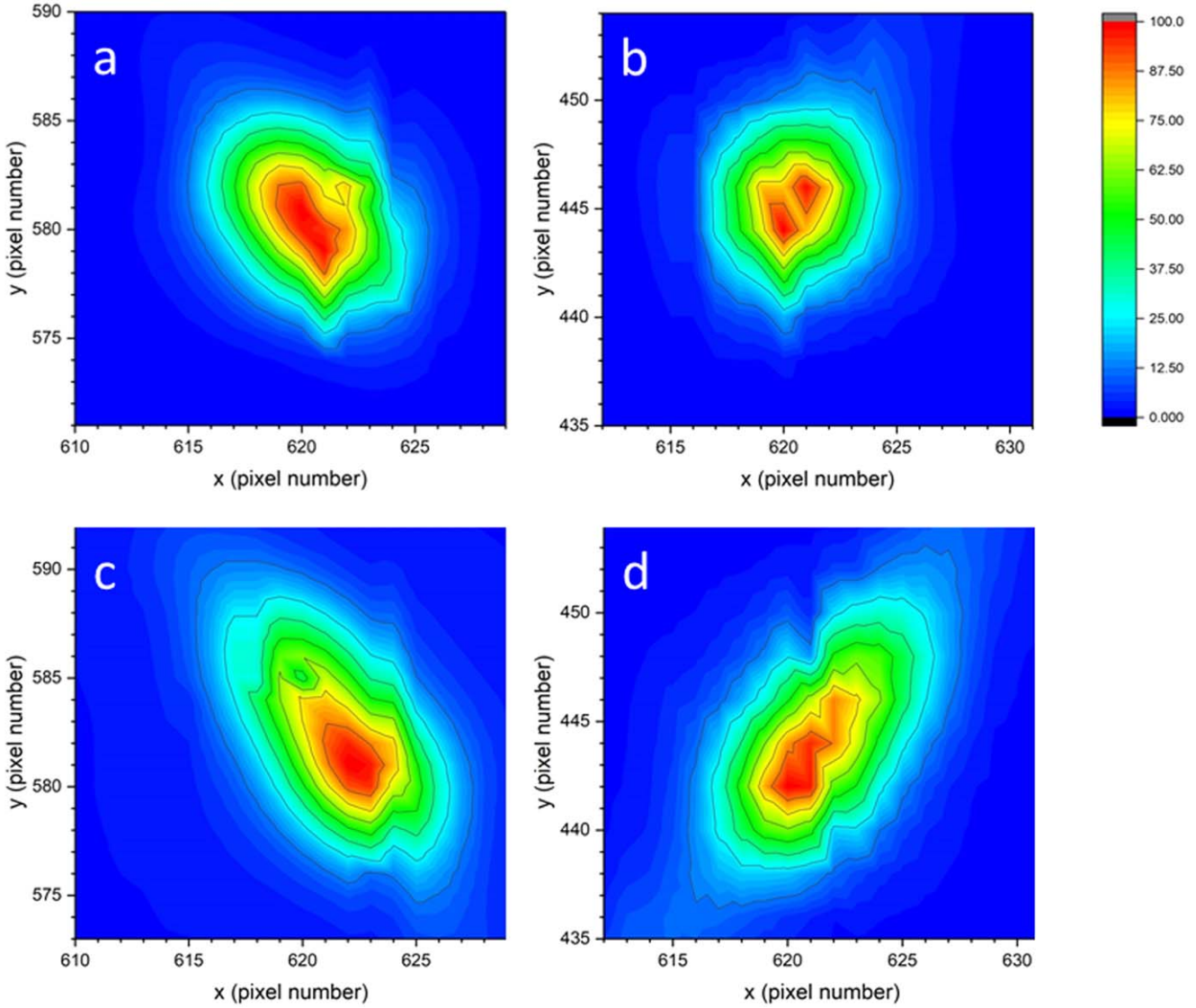


Figure 2. Contour maps of 101 and 10$\bar{1}$ reflections measured at ambient pressure and at 11.1 kbar for $Fe_{0.994}Ni_{0.007}Te_{0.66}Se_{0.34}$ crystal: 110 reflection at ambient (a) and 11.1 kbar (c); 10$\bar{1}$ reflection at ambient (b) and 11.1 kbar (d). The common intensity scale (intensities corresponding to seven contours) is shown at the upper right site. The elongation of the reflection observed in the lower panels indicates that at the indicated pressure the crystal quality is inferior.

homogeneity of the crystal. We have observed that the diffraction quality of the $Fe_{0.994}Ni_{0.007}Te_{0.66}Se_{0.34}$ crystal drops down at 11.1 kbar as compared with that at ambient pressure. The $Fe_{0.994}Ni_{0.007}Te_{0.66}Se_{0.34}$ crystal does not undergo a phase transition at the applied pressure.

3.2. The critical temperature

The dependences of the magnetic susceptibility on temperature in a direct current (dc) field of 10 Oe, parallel to the *c*-axis, determined under ambient pressure and hydrostatic pressure up to 10 kbar, for $FeTe_{0.5}Se_{0.5}$, $Fe_{0.99}Te_{0.66}Se_{0.34}$, and $Fe_{0.994}Ni_{0.007}Te_{0.66}Se_{0.34}$ show a different behavior (cf figures 3(a)–(c)). The critical temperature onset was determined as the point on the *x*-axis where the curve of temperature dependence of magnetization in zero-field-cooling mode, $M_{ZFC}(T)$, deviates from a constant, temperature independent background value. The width of the superconducting transition is almost unaffected by pressure, for the pressures investigated, evidenced by the almost linear dependence of the zero-field-cooling (ZFC) magnetic susceptibility below T_c. A significant divergence between M_{ZFC} and M_{FC} curves points to strong pinning of vortices in both crystals (see figures 3(b) and (c)). The substitution of Ni lowers the critical temperature by 0.9 K at ambient pressure, down to 12 K (compare figures 3(b) and (c)), confirming the recently published data by Bezusyy *et al* [31]. The pressure-induced increase of T_c is clearly observed in the pressure range of 0–10 kbar, for both $Fe_{0.99}Te_{0.66}Se_{0.34}$ (figure 3(b)) and $Fe_{0.994}Ni_{0.007}Te_{0.66}Se_{0.34}$ (figure 3(c)). The rate of increase of T_c in the 0–10 kbar pressure range resembles that for $FeTe_{0.5}Se_{0.5}$ (figure 3(a)). At ambient pressure, the Meissner effect is not completed down to 5 K for $Fe_{0.99}Te_{0.66}Se_{0.34}$, and the application of hydrostatic pressure does not change that trend (figure 3(b)). On the contrary, the Ni-substituted sample shows full Meissner

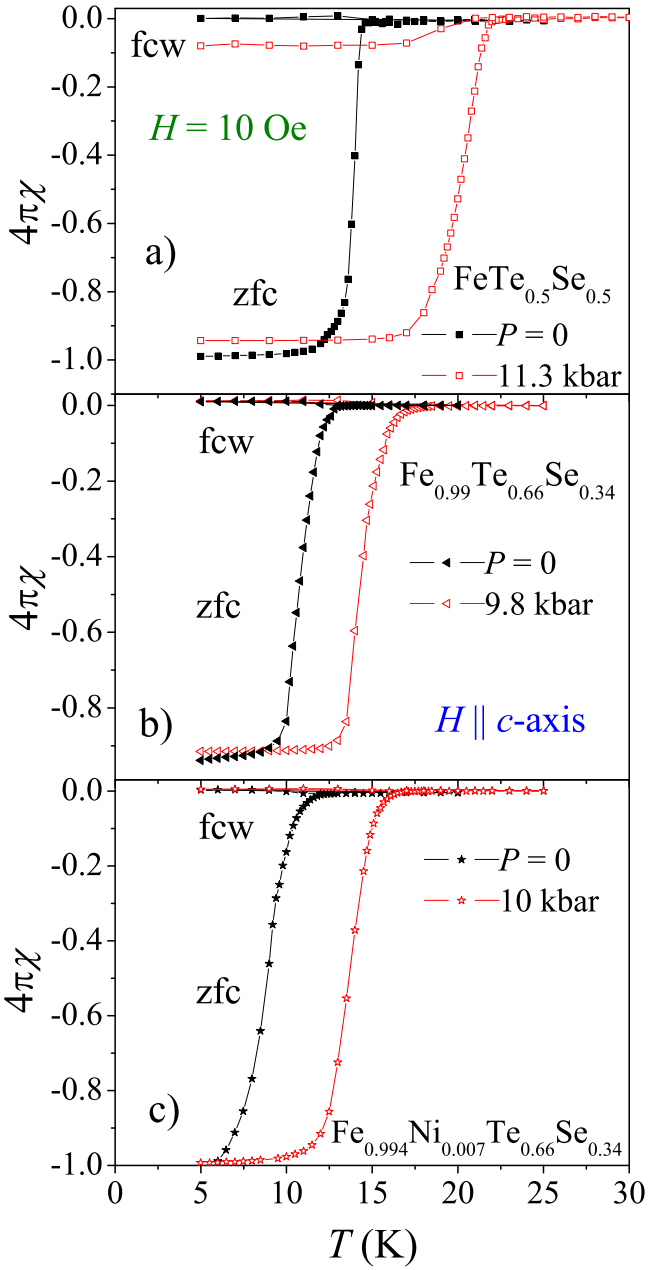


Figure 3. Temperature dependences of the dc magnetic susceptibility for $H||c$-axis, measured under ambient and hydrostatic pressure, in a dc field of 10 Oe, for $FeTe_{0.5}Se_{0.5}$ (a), $Fe_{0.99}Te_{0.66}Se_{0.34}$ (b), and $Fe_{0.994}Ni_{0.007}Te_{0.66}Se_{0.34}$ (c).

effect, regardless of the applied hydrostatic pressure (figure 3(c)). The partial substitution of Fe by Ni was found to suppress superconducting properties, probably as a result of scattering of Cooper pairs, as pointed out by Gawryluk *et al* [23]. It seems that the hydrostatic pressure contributes to weakening of Cooper pairs scattering in $Fe_{0.994}Ni_{0.007}Te_{0.66}Se_{0.34}$, caused by the introduction of nickel ions.

3.3. Basic superconducting parameters—the upper and lower critical fields

In order to compare the superconducting parameters of three single crystals, the earlier reported $FeTe_{0.5}Se_{0.5}$ [20], and the currently studied $Fe_{0.99}Te_{0.66}Se_{0.34}$ and $Fe_{0.994}Ni_{0.007}Te_{0.66}Se_{0.34}$, the dependences of the lower and upper critical fields on temperature in $H||c$-axis geometry (up to 50 kOe) were determined, for the investigated samples under both ambient pressure and a hydrostatic pressure of 10 kbar. The temperature dependence of the magnetic moment, m, for $Fe_{0.994}Ni_{0.007}Te_{0.66}Se_{0.34}$ was recorded under a pressure of 10 kbar for several magnetic fields in $H||c$-axis geometry (see figure 4(a)). Based on these data, the temperature $T_{c2}(H = \text{const.})$, at which $m(T)$ dependence deviates from linear temperature dependence, resembling well the normal state magnetic susceptibility, was determined. The $T_{c2}(H)$ values evaluated in this way for various fields' values permit us to plot the $H_{c2}(T)$ dependences for magnetic field parallel to the c-axis, under ambient pressure and a hydrostatic pressure of 10 kbar.

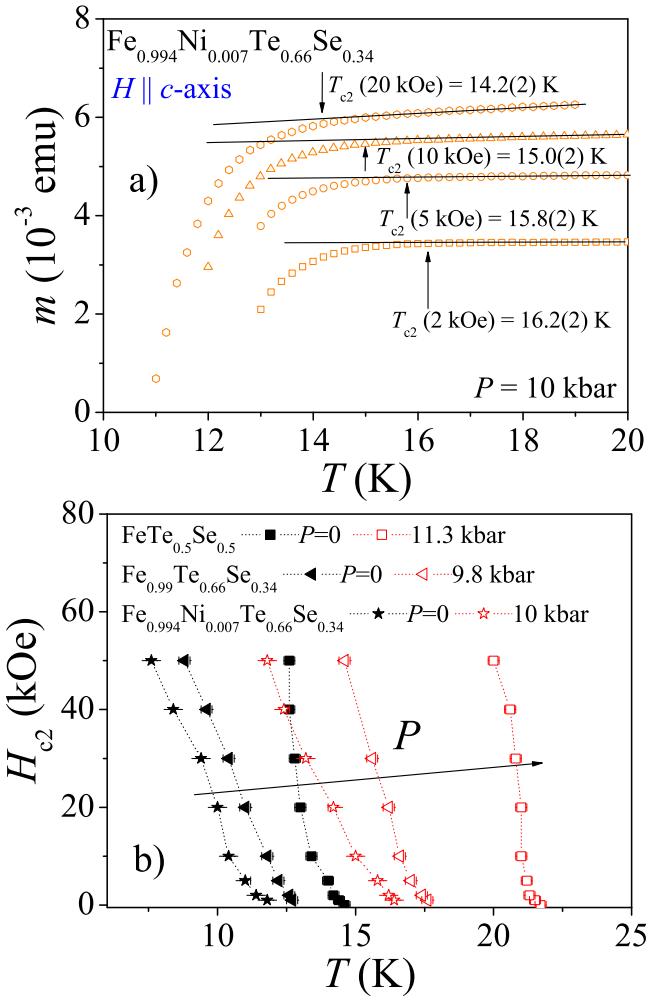


Figure 4. (a) The temperature dependence of the magnetic moment measured for $Fe_{0.994}Ni_{0.007}Te_{0.66}Se_{0.34}$ under an applied hydrostatic pressure of 10 kbar, shown for selected magnetic fields for $H||c$-axis. (b) The temperature dependences of the upper critical field, for $H||c$-axis, for both investigated compounds together with $FeTe_{0.5}Se_{0.5}$ [20] at ambient and at hydrostatic pressures.

The upper critical field temperature dependences for magnetic field parallel to the c-axis ($H_{c2}^{||c}$) for $Fe_{0.99}Te_{0.66}Se_{0.34}$ and $Fe_{0.994}Ni_{0.007}Te_{0.66}Se_{0.34}$, at ambient pressure and under a

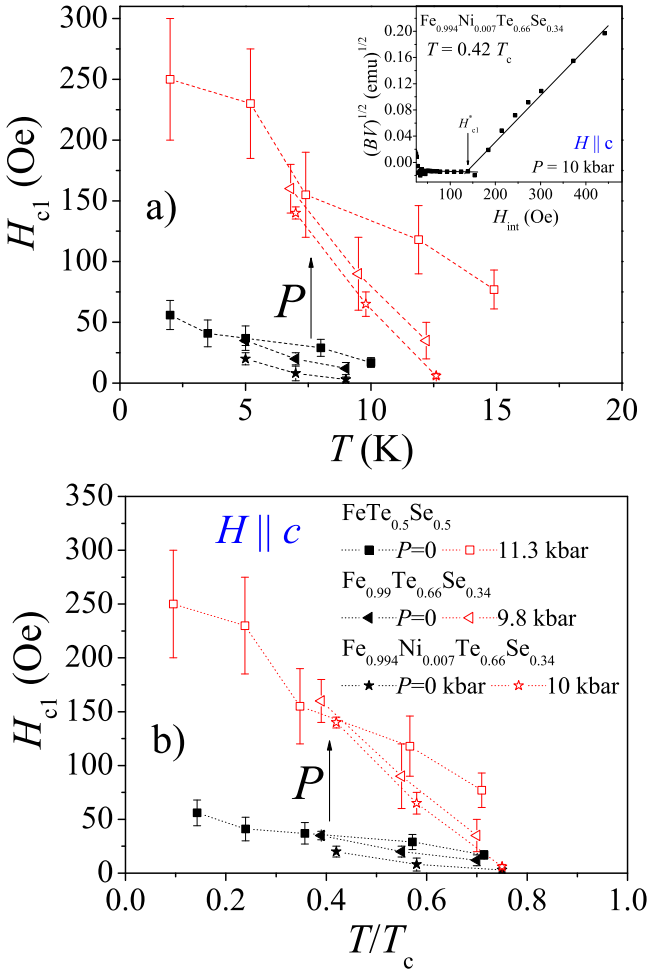


Figure 5. (a) The temperature dependence of H_{c1} for both investigated compounds together with $FeTe_{0.5}Se_{0.5}$ [20] for $H||c$-axis, determined at ambient and at hydrostatic pressure. Inset: values of $(BV)^{1/2}$ as a function of the internal magnetic field, H_{int}, determined at 5 K at hydrostatic pressure of 10 kbar for $Fe_{0.994}Ni_{0.007}Te_{0.66}Se_{0.34}$ for $H||c$-axis. (b) The dependences of the lower critical field on reduced temperature at ambient pressure and under hydrostatic pressures for $H||c$-axis.

nonzero hydrostatic pressure, illustrate the effect of pressure (figure 4(b)). For both $Fe_{0.99}Te_{0.66}Se_{0.34}$ and $Fe_{0.994}Ni_{0.007}Te_{0.66}Se_{0.34}$ compounds, a substantial enhancement of the upper critical field under pressure is apparently visible in this figure. For $Fe_{0.99}Te_{0.66}Se_{0.34}$, a significant enlargement of the slope $-dH_{c2}^{||c}/dT$ in the linear part of the $H_{c2}(T)$ dependence was noticed at higher fields. At lower fields, for temperatures close to T_c, one can notice some curvature, which is not influenced by high hydrostatic pressure. In the case of $Fe_{0.994}Ni_{0.007}Te_{0.66}Se_{0.34}$, for the $H||c$-axis, in the field range between 10 and 50 kOe, we have determined $-dH_{c2}^{||c}/dT = 13.5(1.5)$ kOe/K at ambient pressure, which decreases to 12.0 (5) kOe/K under 10 kbar. For the Ni-substituted compound, the trend of $-dH_{c2}^{||c}/dT(P)$ is opposite with respect to non-substituted $Fe_{0.99}Te_{0.66}Se_{0.34}$ and $FeTe_{0.5}Se_{0.5}$ [20]. The partial substitution of Fe by Ni atoms practically suppresses the curvature of $H_{c2}(T)$ dependence near T_c. Estimating $H_{c2}(0)$ from extrapolations of the present data, recorded in a limited temperature range, is inappropriate not only due to the curvature of $H_{c2}(T)$, but more crucially due to the possible two-band nature of superconductivity. Nevertheless, if one would disregard these considerations, the simple Werthamer–Helfand–Hohenberg (WHH) extrapolation [41] is expected to provide the reliable values of $H_{c2}(0)$.

Whereas the cuprates were characterized by a well-defined effective mass anisotropy, the observation of two distinct anisotropy parameters in MgB_2 challenged the understanding of anisotropic superconductors [42–44]. Various experiments, such as magnetic torque [45, 46], tunneling [47, 48], point contact and infrared spectroscopy [49, 50], as well as the measurements of the specific heat [51], indicate that Fe-based pnictides are multigap superconductors with unconventional anisotropic properties [45, 46], similar to MgB_2 [52, 53]. The multiband nature and its effect on the measured parameters in iron-based superconductors has recently been discussed, especially in the context of high T_c observed in single layers of FeSe, see e.g. [54, 55]. However, in our opinion there is no consensus for multiband superconductivity in selenides. Taking the above into account, the discussions of the effects, being out of the scope of experimental verification with the technique applied in the current manuscript, was intentionally avoided.

From measurements of H_{c2}, the coherence length, ξ_{ab}, was derived using the following formula:

$$H_{c2}^{||c} = \frac{\Phi_0}{2\pi\xi_{ab}^2}, \qquad (1)$$

where Φ_0 represents the elementary flux quantum. Under the assumption that $H_{c2}(0)$ is proportional to both T_c and to $-dH_{c2}/dT$, determined in a relatively wide magnetic field range above the pronounced curvature of $H_{c2}(T)$ near T_c [41], it was estimated that $H_{c2}^{||c}(0) = 120(10)$ kOe under ambient pressure increases up to 240(10) kOe under $P = 9.8$ kbar for $Fe_{0.99}Te_{0.66}Se_{0.34}$. This implies a decrease of the zero-temperature coherence length ξ_{ab} from about 5.2 to 3.7 nm. The minor substitution of Ni does not affect noticeably the value of $H_{c2}^{||c}(0)$, at ambient pressure (=120(10) kOe), when compared to that of $Fe_{0.99}Te_{0.66}Se_{0.34}$. At 10 kbar, $H_{c2}^{||c}(0)$ increases to 150(10) kOe at 10 kbar. This implies a decrease of the zero-temperature coherence length ξ_{ab} from about 5.2 to 4.7 nm.

The lower critical field H_{c1} was estimated following the procedure proposed in [56] and discussed in the studies of superconducting parameters of $FeSe_{0.5}Te_{0.5}$ single crystals under ambient pressure [57] and under hydrostatic pressure [20] (see figure 5(a)). In short, the field dependence of the magnetic moment was measured at various temperatures in the magnetic field oriented parallel to the c-axis of the crystal. For a particular shape of the studied crystal, the demagnetizing factor D was calculated and used for corrections of the values of external magnetic field. The variation of the square root of a product of magnetic induction $B = 4\pi m/V + H_{int}$ and volume of the sample V as a function of the internal magnetic field $H_{int} = H_{ext} - DM$ (H_{ext} denotes the external magnetic field) is presented in the inset of figure 5(a). The lower critical field values $H_{c1}(T)$ for H parallel to the c, presented in figure 5(a), were determined as the field H where the $(BV)^{1/2}$ plotted as a function of H for fixed T deviates from zero value. If bulk

Table 1. The pressure impact on basic superconducting parameters for $Fe_{0.99}Te_{0.66}Se_{0.34}$, $Fe_{0.994}Ni_{0.007}Te_{0.66}Se_{0.34}$, and $FeTe_{0.5}Se_{0.5}$ (after [20]).

	$Fe_{0.99}Te_{0.66}Se_{0.34}$		$Fe_{0.994}Ni_{0.007}Te_{0.66}Se_{0.34}$		$FeTe_{0.5}Se_{0.5}$ [20]	
Quantity	0 kbar	9.8 kbar	0 kbar	10 kbar	0 kbar	11.3 kbar
T_c (K)	12.8(2)	17.6(2)	12.0(2)	16.8(2)	14.2(2)	22.0(2)
$-dH_{c2}^{\|\|c}/dT$ (kOe/K)	13.5(5)	19.5(5)	13.5(1.5)	12.0(5)	45(5)	45(5)
$H_{c2}^{\|\|c}(0)$ (kOe)	120(10)	240(10)	120(10)	150(10)	450(50)	690(80)
$H_{c1}^{\|\|c}(0)$ (Oe)	40(5)	190(10)	25(5)	160(15)	56(8)	250(30)
$\xi_{ab}(0)$ (nm)	5.20(20)	3.70(20)	5.20(20)	4.70(20)	2.70(15)	2.20(15)
$\lambda_{ab}(0)$ (nm)	455(15)	215(20)	585(55)	210(20)	400(50)	180(20)
$\kappa^{\|\|c}(0)$	85(5)	60(10)	110(10)	45(5)	150(20)	80(15)

pinning is weak, surface barriers may play an important role and determine the first field of flux penetration. For investigated samples, magnetization loops are symmetric which means that the bulk pinning mainly has a hold over the entry and exit of the magnetic flux and the impact of surface barriers is insignificant. The H_{c1} values were determined in the same way under ambient and hydrostatic pressure. Hence, one can believe that even if absolute values are determined with some uncertainty, the impact of pressure is established correctly. The reduced temperature dependences of H_{c1} for $H||c$-axis ($H_{c1}^{||c}$) for both investigated compounds, determined at ambient pressure and under a nonzero hydrostatic pressure, are presented in figure 5(b) (the values extrapolated to 0 K are quoted in table 1). The data of H_{c1} for $Fe_{0.994}Ni_{0.007}Te_{0.66}Se_{0.34}$ were collected in the temperature range above the relatively high temperature of 5 K, i.e. $0.42T_c$. However, these data were plotted as a function of reduced transition temperature together with the data for $FeTe_{0.5}Se_{0.5}$ measured down to $0.1T_c$, i.e., to the temperature below 2 K. Since $H_{c1}(T/T_c)$ dependence is similar for both studied compounds, the H_{c1} data for $Fe_{0.994}Ni_{0.007}Te_{0.66}Se_{0.34}$ were extrapolated to $T = 0$. At ambient pressure, the $Fe_{0.99}Te_{0.66}Se_{0.34}$ sample, with larger values of T_c and H_{c2}, is characterized by values of H_{c1} larger than that of $Fe_{0.994}Ni_{0.007}Te_{0.66}Se_{0.34}$. This indicates that the value of penetration depth for $Fe_{0.99}Te_{0.66}Se_{0.34}$ is smaller and the density of superconducting carriers is larger than that of $Fe_{0.994}Ni_{0.007}Te_{0.66}Se_{0.34}$. From the data presented in figure 5, the extrapolated zero-temperature values for $Fe_{0.99}Te_{0.66}Se_{0.34}$ were found to be $H_{c1}^{||c}(0) = 40(5)$ Oe at ambient pressure and $H_{c1}^{||c}(0) = 190(10)$ Oe under a pressure of 9.8 kbar. As expected, the zero-temperature values of the lower critical field for both investigated compounds are smaller with respect to those for $FeTe_{0.5}Se_{0.5}$, obtained in identical magnetic field orientation [20]. The H_{c1} increases considerably under external pressure for both crystals.

The values of the magnetic penetration depth were calculated from the values of H_{c1}, applying the following basic relation [58]:

$$H_{c1}^{||c} = \frac{\Phi_0}{4\pi\lambda_{ab}^2}[\ln(\kappa^{||c}) + 0.5] \quad (2)$$

Here, λ_{ab} denotes the magnetic penetration depth related to the superconducting current flowing in the *ab*-plane, $\kappa^{||c} = \lambda_{ab}/\xi_{ab}$ is the corresponding Ginzburg–Landau parameter. The zero-temperature value of $\xi_{ab}(0)$ was derived from the value of $H_{c2}^{||c}(T)$ extrapolated to 0 K. The following values of the magnetic penetration depths, $\lambda_{ab}(0)$, at ambient pressure were obtained: 455(15) nm for $Fe_{0.99}Te_{0.66}Se_{0.34}$ and 585(55) nm for $Fe_{0.994}Ni_{0.007}Te_{0.66}Se_{0.34}$. The corresponding values of the penetration depth, $\lambda_{ab}(0)$, at a hydrostatic pressure of about 10 kbar are equal to 215(20) nm for $Fe_{0.99}Te_{0.66}Se_{0.34}$ and 210 (20) nm for $Fe_{0.994}Ni_{0.007}Te_{0.66}Se_{0.34}$. In one of our earlier papers [20], we presented quite similar dependence for $H_{c1}(T)$ and corresponding substantial change of the penetration depth. This is apparently correlated with a large increase of T_c under hydrostatic pressure. The involved microscopic mechanism responsible for this behavior is not clear to us at the present stage. However, observed changes of T_c and superconducting state parameters appear to be correlated with the evolution of crystal quality under pressure. The obtained data reveal the improvement of superconducting parameters observed in Fe(Te,Se), despite the chemical substitutions at Fe- and Te-sites, which contribute to weakening the superconductivity in $Fe_{0.99}Te_{0.66}Se_{0.34}$ and in $Fe_{0.994}Ni_{0.007}Te_{0.66}Se_{0.34}$ at ambient pressure [12, 23, 59]. The values of the basic superconducting parameters under pressure for both the studied samples, together with $FeTe_{0.5}Se_{0.5}$ values as a reference, are given in table 1.

3.4. The critical current density

Flux pinning properties of Fe(Se,Te) have been studied by several authors, see for example [60–62] and recent studies by Galluzzi *et al* [63]. We performed studies into the impact of pressure on the critical current densities (j_c) of both $Fe_{0.99}Te_{0.66}Se_{0.34}$ and $Fe_{0.994}Ni_{0.007}Te_{0.66}Se_{0.34}$ compounds. The j_c values were determined from $M(H)$ dependences, at ambient and at hydrostatic pressure, obtained for selected reduced temperatures, using Bean's model [64, 65]. In the case of $H||c$, we have $j_c^a = j_c^b = j_c^{ab}$, where current flows in the *ab* plane with the dimensions $a = b = 0.12$ cm for $Fe_{0.99}Te_{0.66}Se_{0.34}$ and with the dimensions $a = 0.10$ cm and $b = 0.11$ cm for $Fe_{0.994}Ni_{0.007}Te_{0.66}Se_{0.34}$. The following formula was used to derive the critical current density, j_c^{ab}:

$$j_c^{ab} = \frac{30\Delta M}{a} \quad (3)$$

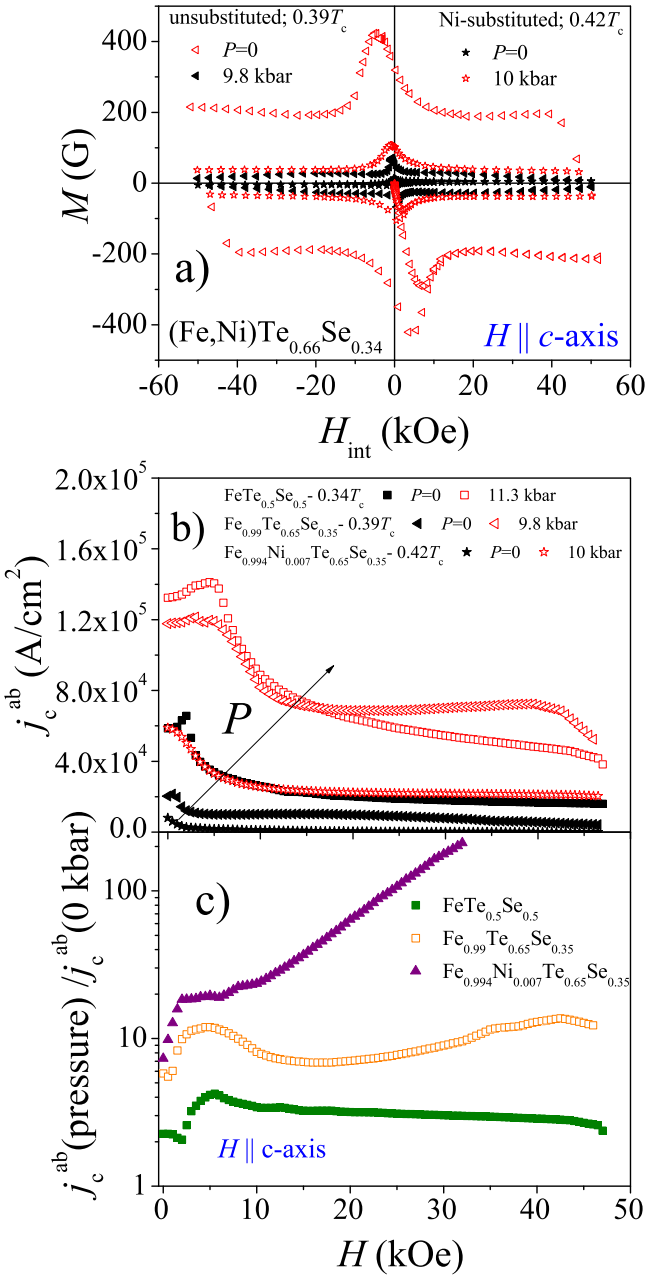


Figure 6. (a) Hysteresis loops of a single crystal of $Fe_{0.99}Te_{0.66}Se_{0.34}$ and $Fe_{0.994}Ni_{0.007}Te_{0.66}Se_{0.34}$ for $H||c$-axis, recorded at 5 K and at 6.8 K at ambient and hydrostatic pressures of 9.8 and 10 kbar, respectively. (b) Dependence of the critical current density on magnetic field, for $H||c$-axis, at ambient and at hydrostatic pressure, for $FeTe_{0.5}Se_{0.5}$, $Fe_{0.99}Te_{0.66}Se_{0.34}$, and $Fe_{0.994}Ni_{0.007}Te_{0.66}Se_{0.34}$, at T/T_c equal to of 0.34, 0.39, and 0.42 respectively. (c) Dependence of the enhancement of the critical current density on field under pressure (the ratio of the critical current densities under ~10 kbar and at ambient pressure), in magnetic field $H||c$-axis, for $FeTe_{0.5}Se_{0.5}$, $Fe_{0.99}Te_{0.66}Se_{0.34}$, and $Fe_{0.994}Ni_{0.007}Te_{0.66}Se_{0.34}$, at T/T_c equal to of 0.34, 0.39, and 0.42, respectively.

Here, ΔM (in oersteds) is the width of the hysteresis loop for increasing and decreasing H_{int} (see figure 6(a)), the current densities are in A cm^{-2}. The dependence of the critical current density for both investigated compounds at ambient and at hydrostatic pressure, calculated according to equation (3), for proper reduced temperatures in the magnetic field geometries $H||c$-axis, is presented in figure 6(b). For both investigated samples, we found an increase in critical current density under pressure. The disorder introduced into the sublattice of magnetic ions, caused by partial substitution of Fe by Ni, leads to a reduction of the estimated critical current density, j_c, modestly, when compared to both undoped $FeTe_{1-x}Se_x$ samples.

The dependence of the enlargement of the critical current density on magnetic field under pressure (the ratio of j_c under hydrostatic and at ambient pressure) at reduced temperatures T/T_c equal to 0.34, 0.39, and 0.42 for $FeTe_{0.5}Se_{0.5}$, $Fe_{0.99}Te_{0.66}Se_{0.34}$, and $Fe_{0.994}Ni_{0.007}Te_{0.66}Se_{0.34}$, respectively, is presented in figure 6(c). The Ni-containing sample was found to have the biggest improvement of critical current density under pressure by more than one order of magnitude in the full magnetic field range. The pressure enhancement of j_c is evidently stronger by up to two orders of magnitude at higher magnetic fields. This is related to a significant increase of H_{c2} under pressure.

The increase in critical current density under pressure is related to the increasing effectiveness of small pinning centers in the sample under pressure. This effect is due to a reduction in the coherence length under pressure, and because of an enhancement of the thermodynamic critical field under pressure as a consequence of the increase in both the upper and the lower critical fields.

4. Conclusions

The complex relationship between the structure, magnetism, and superconductivity in $Fe_{0.994}Ni_{0.007}Te_{0.66}Se_{0.34}$ and $Fe_{0.99}Te_{0.66}Se_{0.34}$ crystals of iron selenides, at ambient pressure and under hydrostatic pressure, was studied as external pressure enables the control of many physical properties. The superconducting-state properties of the single phase $Fe_{0.99}Te_{0.66}Se_{0.34}$ crystal, such as lower and upper critical fields, were found to be poorer at both ambient and hydrostatic pressure than those observed for the multiphase $FeTe_{0.5}Se_{0.5}$ sample. However, the recovery of superconducting state properties was not observed in the $Fe_{0.994}Ni_{0.007}Te_{0.66}Se_{0.34}$ crystal as a result of disorder introduced by Ni substitution, as compared with those in $Fe_{0.99}Te_{0.66}Se_{0.34}$. It means that a nonhomogeneous spatial spreading of ions with nanoscale phase separation is essential for the enhancement of superconductivity, but disorder introduced by simple substitution of another kind of ions alone is not sufficient. The critical current density at ambient pressure is much smaller for $Fe_{0.994}Ni_{0.007}Te_{0.66}Se_{0.34}$ than that for both $Fe_{0.99}Te_{0.66}Se_{0.34}$ and $FeTe_{0.5}Se_{0.5}$, but under hydrostatic pressure the Ni-substituted sample has greater enlargement of the critical current density than that for both $Fe_{0.99}Te_{0.66}Se_{0.34}$ and $FeTe_{0.5}Se_{0.5}$ samples. For $Fe_{0.994}Ni_{0.007}Te_{0.66}Se_{0.34}$, the x-ray diffraction studies have revealed a degradation of crystal quality under applied

elevated pressure. Observation of diffraction-spot-shape variation for $Fe_{0.994}Ni_{0.007}Te_{0.66}Se_{0.34}$ under pressure, attributed to increase in mosaicity, correlates with the observed pressure-induced enhancement of superconductive properties. The increase in mosaicity is a possible explanation for the earlier observation of the variation in superconducting properties in related sulpho-iron seleno-tellurides of anti-PbO-type structure. On returning to ambient pressure, all of the samples' parameters recovered their ambient pressure values.

Acknowledgments

This work was partially supported by the National Science Centre of Poland based on decision No. DEC-2013/08/M/ST3/00927. DP is especially grateful for the support from Miniatura Grant (decision No. 2018/02/X/ST3/02880), funded by the National Science Centre.

ORCID iDs

Jaroslaw Pietosa https://orcid.org/0000-0002-0824-5120
Roman Puzniak https://orcid.org/0000-0001-5636-5541
Andrzej Katrusiak https://orcid.org/0000-0002-1439-7278
Radosław Kamiński https://orcid.org/0000-0002-8450-0955
Andrzej Wisniewski https://orcid.org/0000-0001-5040-0481

References

[1] Hsu F-C *et al* 2008 *Proc. Natl. Acad. Sci. USA* **105** 14262
[2] Fang M H, Pham H M, Qian B, Liu T J, Vehstedt E K, Liu Y, Spinu L and Mao Z Q 2008 *Phys. Rev. B* **78** 224503
[3] Bao W *et al* 2009 *Phys. Rev. Lett.* **102** 247001
[4] Yeh K-W *et al* 2008 *Eur. Phys. Lett.* **84** 37002
[5] Khasanov R *et al* 2009 *Phys. Rev. B* **80** 140511
[6] Hunte F, Jaroszynski J, Gurevich A, Larbalestier D C, Jin R, Sefat A S, McGuire M A, Sales B C, Christen D K and Mandrus D 2008 *Nature* **453** 903
[7] Yamamoto A *et al* 2009 *Appl. Phys. Lett.* **94** 062511
[8] Khim S, Kim J W, Choi E S, Bang Y, Nohora M, Takagi H and Kim K H 2010 *Phys. Rev. B* **81** 184511
[9] Si W, Zhou J, Jie Q, Dimitrov I, Solovyov V, Johnson P D, Jaroszynski J, Matias V, Sheehan C and Li Q 2011 *Appl. Phys. Lett.* **98** 262509
[10] Mizuguchi Y, Deguchi K, Tsuda S, Yamaguchi T, Takeya H, Kumakura H and Takano Y 2009 *Appl. Phys. Express* **2** 083004
[11] Mele P 2012 *Sci. Technol. Adv. Mater.* **13** 054301
[12] Toshinori O, Keita D, Yoshikazu M, Hiroaki K and Yoshihiko T 2011 *IEEE Trans. Appl. Supercond.* **21** 2858
[13] Liu D *et al* 2012 *Nature Commun.* **3** 931
[14] He S L *et al* 2013 *Nature Mater.* **12** 605
[15] Tan S Y *et al* 2013 *Nature Mater.* **12** 634
[16] Peng R *et al* 2014 *Nature Commun.* **5** 5044
[17] Ge J F, Liu Z L, Liu C, Gao C L, Qian D, Xue Q K, Liu Y and Jia J F 2015 *Nature Mater.* **14** 285
[18] Lee J J *et al* 2014 *Nature* **515** 245
[19] Zhang P *et al* 2018 *Science* **360** 182
[20] Pietosa J, Gawryluk D J, Puzniak R, Wisniewski A, Fink-Finowicki J, Kozlowski M and Berkowski M 2012 *J. Phys.: Condens. Matter* **24** 265701
[21] Sales B C, Sefat A S, McGuire M A, Jin R Y, Mandrus D and Mozharivskyj Y 2009 *Phys. Rev. B* **79** 094521
[22] Lumsden M D *et al* 2010 *Nature Phys.* **6** 182
[23] Gawryluk D J, Fink-Finowicki J, Wisniewski A, Puzniak R, Domukhovski V, Diduszko R, Kozłowski M and Berkowski M 2011 *Supercond. Sci. Technol.* **24** 065011
[24] Wittlin A, Aleshkevych P, Przybylinska H, Gawryluk D J, Dłuzewski P, Berkowski M, Puzniak R, Gutowska M U and Wisniewski A 2012 *Supercond. Sci. Technol.* **25** 065019
[25] Hu H, Zuo J-M, Wen J, Xu Z, Lin Z, Li Q, Gu G, Park W K and Greene L H 2011 *New J. Phys.* **13** 053031
[26] Mizuguchi Y and Takano Y 2010 *J. Phys. Soc. Jap.* **79** 102001
[27] Deguchi K, Takano Y and Mizuguchi Y 2012 *Sci. Technol. Adv. Mater.* **13** 054303
[28] Krzton-Maziopa A, Svitlyk V, Pomjakushina E, Puzniak R and Conder K 2016 *J. Phys.: Condens. Matter* **28** 293002
[29] Bezusyy V L, Gawryluk D J, Berkowski M and Cieplak M Z 2012 *Acta Phys. Pol. A* **121** 816
[30] Bezusyy V L, Gawryluk D J, Malinowski A, Berkowski M and Cieplak M Z 2014 *Acta Phys. Pol. A* **126** 76
[31] Bezusyy V L, Gawryluk D J, Malinowski A and Cieplak M Z 2015 *Phys. Rev. B* **91** 100502 (R)
[32] Merrill L and Bassett W A 1974 *Rev. Sci. Instrum.* **45** 290
[33] Katrusiak A 2004 *Z. Kristallogr.* **219** 461
[34] Murata K, Yoshino H, Yadav H O, Honda Y and Shirakava N 1997 *Rev. Sci. Instrum.* **68** 2490
[35] Kamarad J, Machatova A and Arnold Z 2004 *Rev. Sci. Instrum.* **75** 5022
[36] Gresty N C *et al* 2009 *J. Am. Chem. Soc.* **131** 16944
[37] Malavi P S, Karmakar S, Patel N N, Bhatt H and Sharma S M 2014 *J. Phys.: Condens. Matter* **26** 125701
[38] Bendele M, Guguchia Z, von Rohr F, Irifune T, Shinmei T, Kantor I, Pascarelli S, Joseph B and Marini C 2014 *Phys. Rev. B* **90** 174505
[39] Jha R, Zargar R A, Hafiz A K, Kishan H and Awana V P S 2014 *J. Supercond. Nov. Magn.* **27** 1599
[40] Shylin S I *et al* 2017 *Phys. Status Solidi B* **254** 1600161
[41] Werthamer N R, Hefland E and Hohenberg P C 1966 *Phys. Rev.* **147** 295
[42] Fletcher J D, Carrington A, Taylor O J, Kazakov S M and Karpinski J 2005 *Phys. Rev. Lett.* **95** 097005
[43] Angst M, Puzniak R, Wisniewski A, Jun J, Kazakov S M, Karpinski J, Roos J and Keller H 2002 *Phys. Rev. Lett.* **88** 167004
[44] Angst M and Puzniak R 2004 *Focus on Superconductivity* ed B P Martins vol 1 (New York: Nova Science Publishers) p 1
[45] Weyeneth S, Puzniak R, Mosele U, Zhigadlo N D, Katrych S, Bukowski Z, Karpinski J, Kohout S, Roos J and Keller H 2009 *J. Supercond. Novel Magn.* **22** 325
[46] Weyeneth S, Puzniak R, Zhigadlo N D, Katrych S, Bukowski Z, Karpinski J and Keller H 2009 *J. Supercond. Novel Magn.* **22** 347
[47] Gonnelli R S, Daghero D, Tortello M, Ummarino G A, Stepanov V A, Kremer R K, Kim J S, Zhigadlo N D and Karpinski J 2009 *Physica C* **469** 512
[48] Samuely P, Pribulová Z, Szabó P, Pristáš G, Bud'ko S L and Canfield P C 2009 *Physica C* **469** 507
[49] Szabó P, Pribulová Z, Pristáš G, Bud'ko S L, Canfield P C and Samuely P 2009 *Phys. Rev. B* **79** 012503
[50] Li G, Hu W Z, Dong J, Li Z, Zheng P, Chen G F, Luo J L and Wang N L 2008 *Phys. Rev. Lett.* **101** 107004
[51] Mu G, Luo H, Wang Z, Shan L, Ren C and Wen H H 2009 *Phys. Rev. B* **79** 174501

[52] Nagamatsu J, Nakagawa N, Muranaka T, Zenitani Y and Akimitsu J 2001 *Nature* **410** 63
[53] Gonnelli R S, Daghero D, Ummarino G A, Stepanov V A, Jun J, Kazakov S M and Karpinski J 2002 *Phys. Rev. Lett.* **89** 247004
[54] Defa L *et al* 2012 *Nat. Commun.* **3** 931
[55] Zhao L *et al* 2016 *Nat. Commun.* **7** 10608
[56] Naito M, Matsuda A, Kitazawa K, Kambe S, Tanaka I and Kojami H 1990 *Phys. Rev. B* **41** 4823
[57] Bendele M *et al* 2010 *Phys. Rev. B* **81** 224520
[58] Tinkham M 1975 *Introduction to Superconductivity* (Malabar, FL: Klieger)
[59] Sivakov A G *et al* 2017 *Supercond. Sci. Technol.* **30** 015018
[60] Wu Z F, Wang Z H, Tao J, Qiu L, Yang S G and Wen H H 2016 *Supercond. Sci. Technol.* **29** 035006
[61] Amigó M L, Ale Crivillero M V, Franco D G, Badía–Majós A, Guimpel J, Campo J, Damay F, Porcher F, Condó A M and Nieva G 2017 *Supercond. Sci. Technol.* **30** 085010
[62] Galluzzi A, Buchkov K, Tomov V, Nazarova E, Leo A, Grimaldi G, Nigro A, Pace S and Polichetti M 2018 *Supercond. Sci. Technol.* **31** 015014
[63] Galluzzi A, Buchkov K, Nazarova E, Tomov V, Grimaldi G, Leo A, Pace S and Polichetti M 2019 *Nanotechnology* **30** 254001
[64] Bean C P 1962 *Phys. Rev. Lett.* **8** 250
[65] Bean C P 1964 *Rev. Mod. Phys.* **36** 31